Electronic Supplementary Material

Journal: Molecular Imaging and Biology

[^{18}F]FE-OTS964: A TOPK Inhibitor for *In Vivo* PET Imaging in Mouse Brain Cancer Model

Giacomo Pirovano[1], Sheryl Roberts[1], Christian Brand[1], Patrick L. Donabedian[1], Christian Mason[1], Paula Demétrio de Souza[1], Geoff S. Higgins[2], Thomas Reiner[1,3,*]

[1] Department of Radiology, Memorial Sloan-Kettering Cancer Center, New York, NY, USA

[2] CRUK/MRC Oxford Institute for Radiation Oncology, University of Oxford, Oxford, UK

[3] Department of Radiology, Weill Cornell Medical College, New York, NY, USA

***Corresponding author:**
Thomas Reiner, Ph.D.
Department of Radiology, MSK
1275 York Avenue
New York, NY 10065
Phone: 646-888-3461
Fax: 646-422-0408
Email: reinert@mskcc.org

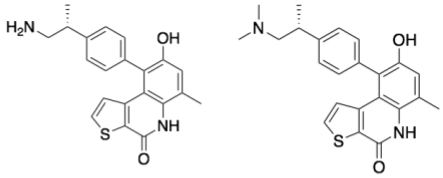

	OTS514	OTS964
TOPK IC50 (nM)	2.6	32
MW (g/mol)	364.46	392.52
clogP (calc)	2.95	3.63

Fig. S1: Structures and relevant physicochemical parameters of OTS514 and OTS964.

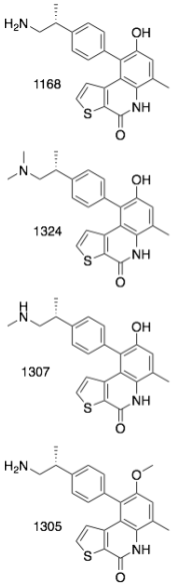

IC_{50} (nM):	PBK	BT549	T47D	A549	HT1197
OTS514	2.6	-	8.4	6.5	27
OTS964	32	30	66	24	69
OTS514-NMe	18	42	85	57	150
OTS514-OMe	15	21	40	20	64

Fig. S2: Structures of OTS514 and OTS964 and relevant physicochemical parameters

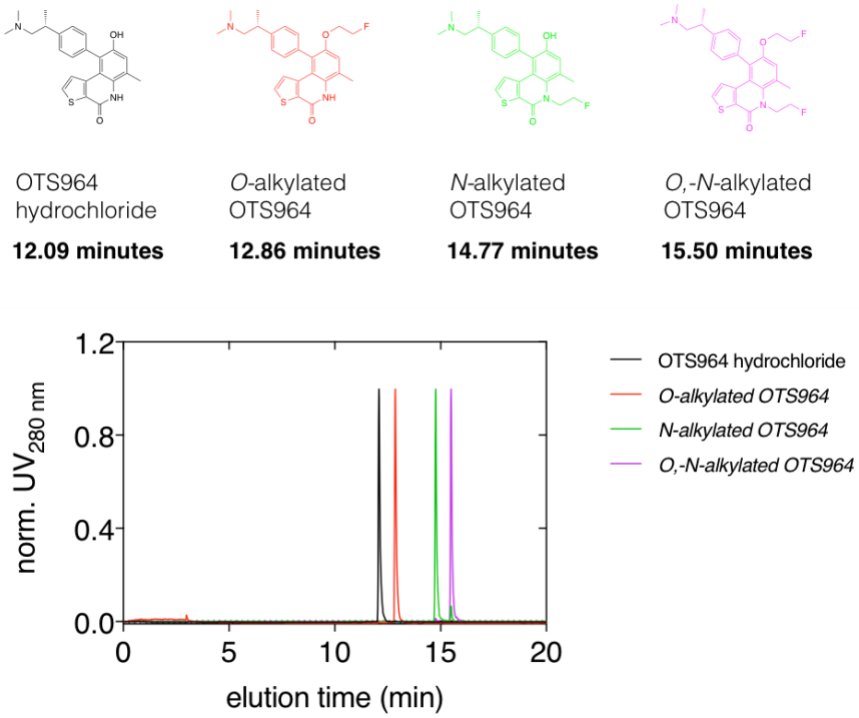

Fig. S3: QC normalized chromatograms of (left to right) OTS964 hydrochloride, *O*-alkylated OTS964, *N*-alkylated OTS964, and *O*-,*N*-alkylated OTS964

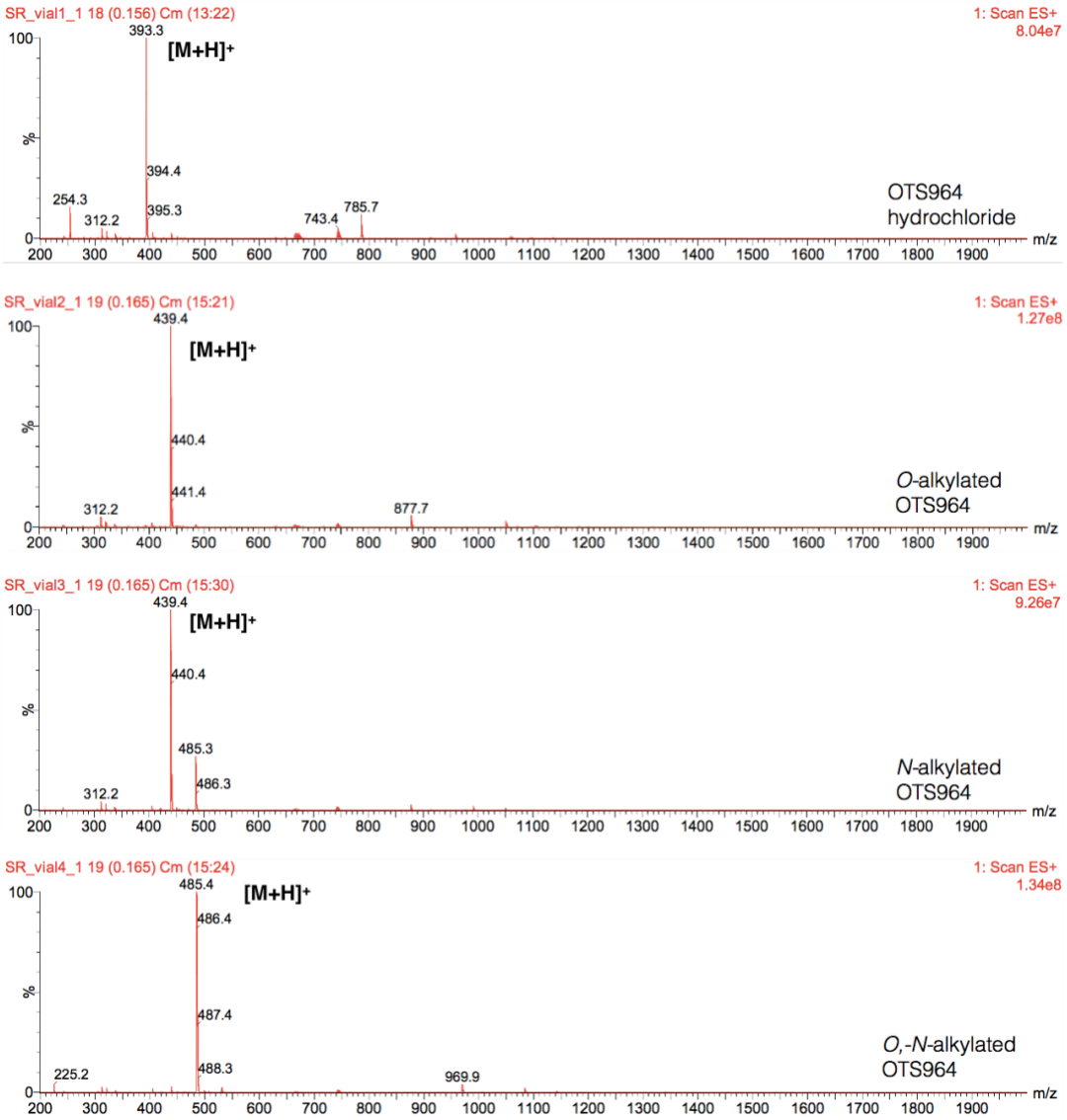

Fig. S4: LC-MS chemical identification of (top to bottom) OTS964 hydrochloride, *O*-alkylated OTS964, *N*-alkylated OTS964, and *O*-,*N*-alkylated OTS964

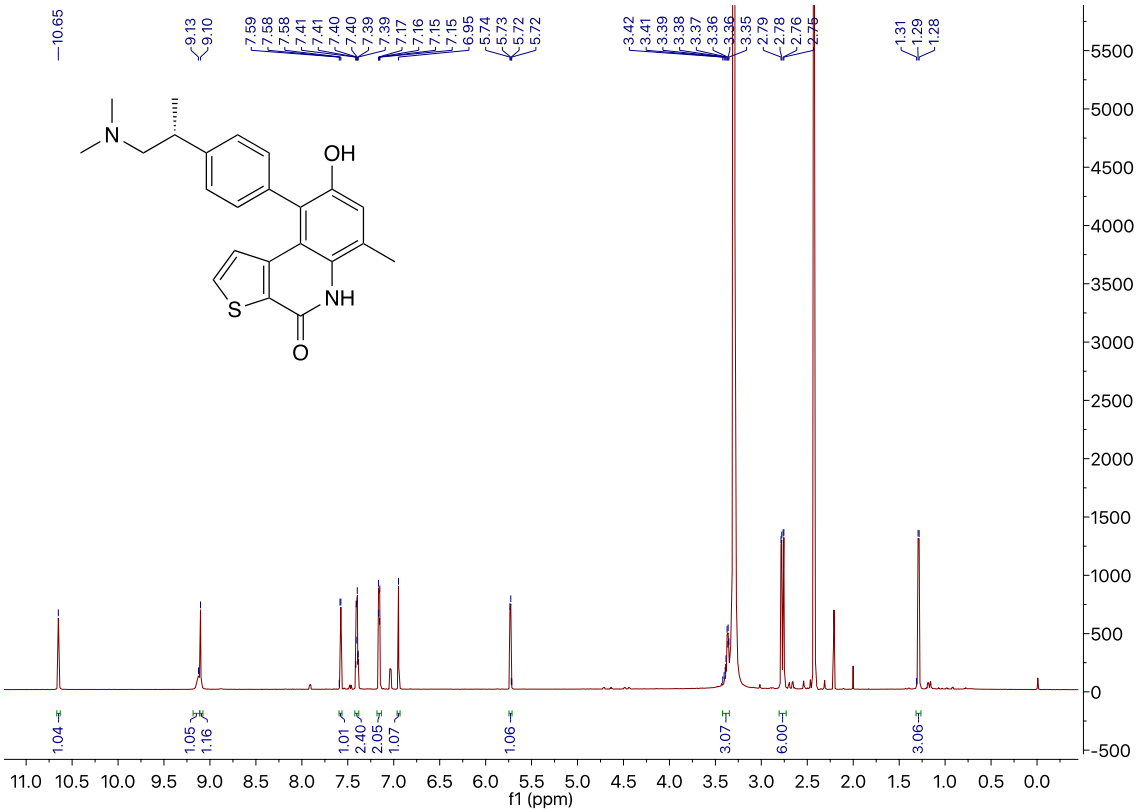

Fig. S5: ^{1}H NMR of OTS964. ^{1}H NMR (DMSO-d6, 600 MHz): δ 10.65 (s, 1H, -N(CH$_3$)$_2$H$^+$, 9.13 (s, 1H, Ar-NH), 9.10 (s, 1H, -OH), 7.58 (d, J = 5.4 Hz, 1H, -CHCHS), 7.42 – 7.38 (m, 2H, -CH^{Ar}), 7.18 – 7.13 (m, 2H, -CH^{Ar}), 6.95 (s, 1H, -CH^{Ar}), 5.73 (d, J = 5.4 Hz, 1H, -CHCHS), 3.42 – 3.35 (m, 3H, Ar-CH(CH$_3$)CH$_2$-), 2.77 (dd, J = 13.8, 4.8 Hz, 6H, -N(CH$_3$)$_2$), 2.43 (s, 3H, -Ar-CH$_3$) 1.29 (d, J = 6.8 Hz, 3H, -CH$_3$). Identity by LC-MS analysis, ESI-MS (ES$^+$) calculated for $C_{23}H_{24}FN_2O_2S$ [M+H]$^+$ m/z 393.30, found 393.16

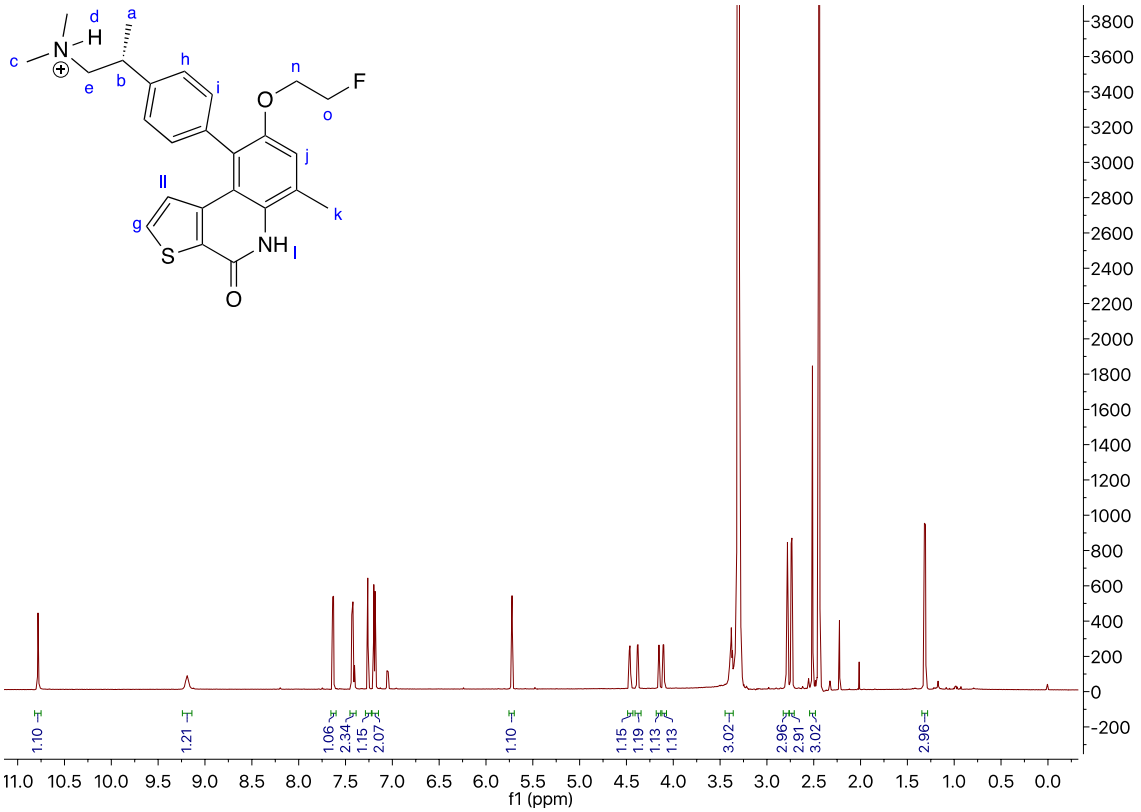

Fig. S6: ^{1}H NMR of *O*-alkylated OTS964. ^{1}H NMR (DMSO-d6, 600 MHz): δ 10.78 (s, 1H, -N(CH$_3$)$_2$H$^+$), 9.19 (s, 1H, Ar-NH), 7.63 (d, *J* = 5.4 Hz, 1H, -CHCHS), 7.45– 7.39 (m, 2H, -CH^{Ar}), 7.26 (s, 1H, -CH^{Ar}), 7.22 – 7.15 (m, 2H, -CH^{Ar}), 5.73 (d, *J* = 5.4 Hz, 1H, -CHCHS), 4.42 (ddd, *J* = 47.8, 7.5, 3.8 Hz, 2H, -OCH$_2$CH$_2$F), 4.13 (ddd, *J* = 30.2, 4.5, 3.2 Hz, 2H, -OCH$_2$CH$_2$F), 3.46 – 3.36 (m, 3H, Ar-CH(CH$_3$)CH$_2$-), 2.76 (dd, *J* = 28.7, 4.8 Hz, 6H, -N(CH$_3$)$_2$), 2.51 (s, 3H, Ar-CH$_3$), 1.31 (d, *J* = 6.7 Hz, 3H, -CH$_3$). Identity by LC-MS analysis, ESI-MS (ES$^+$) calculated for $C_{25}H_{27}FN_2O_2S$ [M+H]$^+$ m/z 439.4, found 439.18

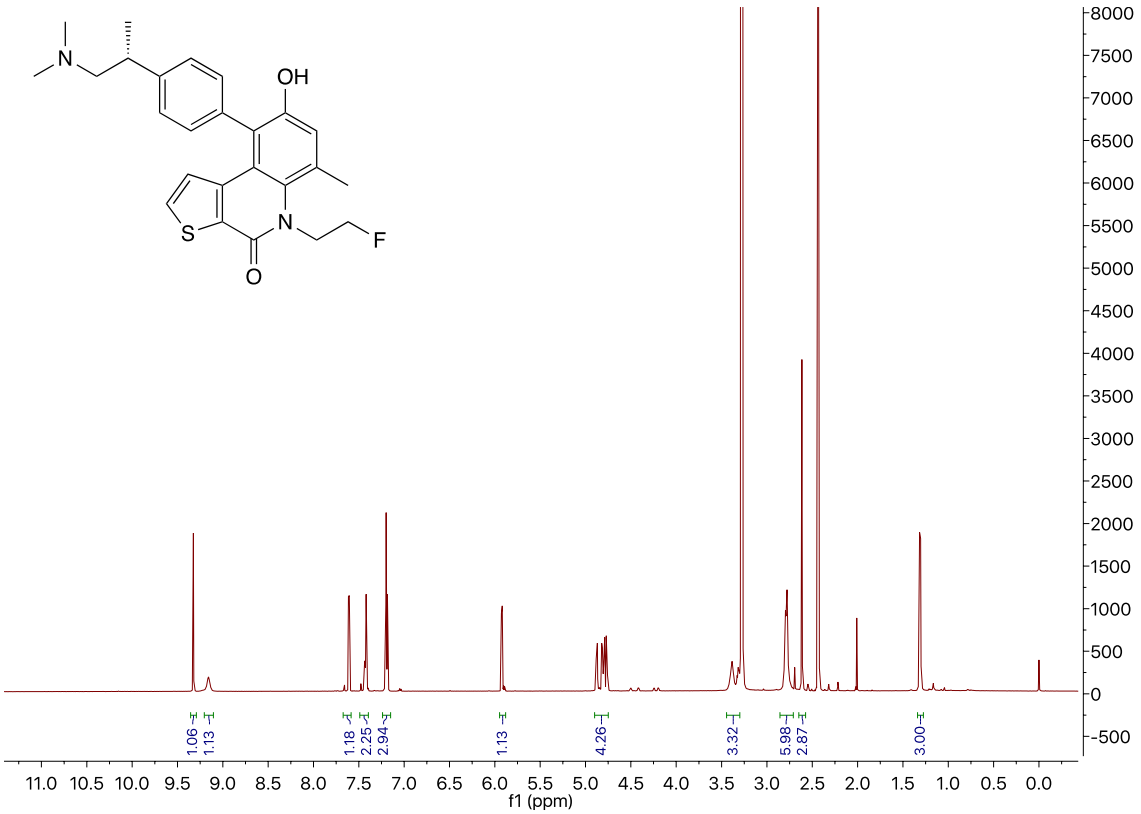

Fig. S7: ^{1}H NMR of *N*-alkylated OTS964. ^{1}H NMR (600 MHz, DMSO-d_6) δ 9.32 (s, 1H, -N(CH$_3$)$_2$<u>H</u>$^+$), 9.16 (s, 1H, -OH), 7.61 (d, *J* = 5.5 Hz, 1H, -CHC<u>H</u>S), 7.43 (d, *J* = 7.7 Hz, 2H, -C<u>H</u>^{Ar}), 7.24 – 7.15 (m, 3H, -C<u>H</u>^{Ar}), 5.92 (d, *J* = 5.5 Hz, 1H, -C<u>H</u>CHS), 4.91 – 4.73 (m, 4H, -NC<u>H</u>$_2$C<u>H</u>$_2$F), 3.45 – 3.30 (m, 3H, Ar-C<u>H</u>(CH$_3$)C<u>H</u>$_2$-), 2.86 – 2.71 (m, 6H, -N(C<u>H</u>$_3$)$_2$), 2.65 – 2.57 (m, 3H, Ar-C<u>H</u>$_3$), 1.31 (d, *J* = 6.7 Hz, 3H, -C<u>H</u>$_3$). Identity by LC-MS analysis, ESI-MS (ES$^+$) calculated for $C_{25}H_{27}FN_2O_2S$ [M+H]$^+$ m/z 439.40, found 439.18

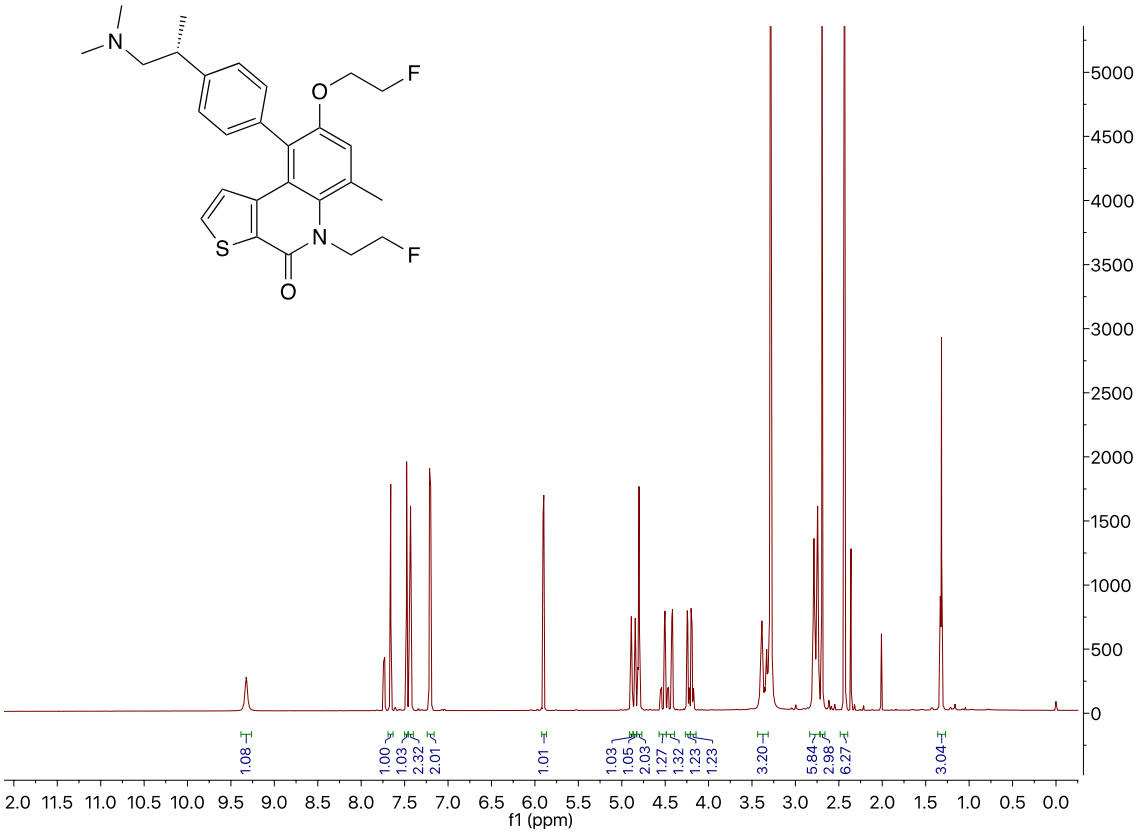

Fig. S8: ^{1}H NMR of *O-,N*-alkylated OTS964. ^{1}H NMR (600 MHz, DMSO-d_6) δ 9.33 (d, J = 11.2 Hz, 1H, -N(CH$_3$)$_2$H$^+$), 7.66 (d, J = 5.5 Hz, 1H, -CHCHS), 7.48 (s, 1H, -CH^{Ar}), 7.43 (m, 2H, -CH^{Ar}), 7.24 – 7.16 (m, 2H, -CH^{Ar}), 5.90 (d, J = 5.5 Hz, 1H, -CHCHS), 4.92 – 4.83 (m, 2H, -NCH$_2$CH$_2$F), 4.83 – 4.77 (m, 2H, -NCH$_2$CH$_2$F), 4.57 – 4.39 (m, 2H, -OCH$_2$CH$_2$F), 4.27 – 4.14 (m, 2H, -OCH$_2$CH$_2$F), 3.36 (m, 3H, Ar-CH(CH$_3$)CH$_2$-), 2.77 (d, J = 25.1 Hz, 6H, -N(CH$_3$)$_2$), 2.69 (s, 3H, Ar-CH$_3$), 1.32 (d, J = 6.7 Hz, 3H, -CH$_3$). Identity by LC-MS analysis, ESI-MS (ES$^+$) calculated for $C_{27}H_{30}F_2N_2O_2S$ [M+H]$^+$ m/z 485.40, found 485.20

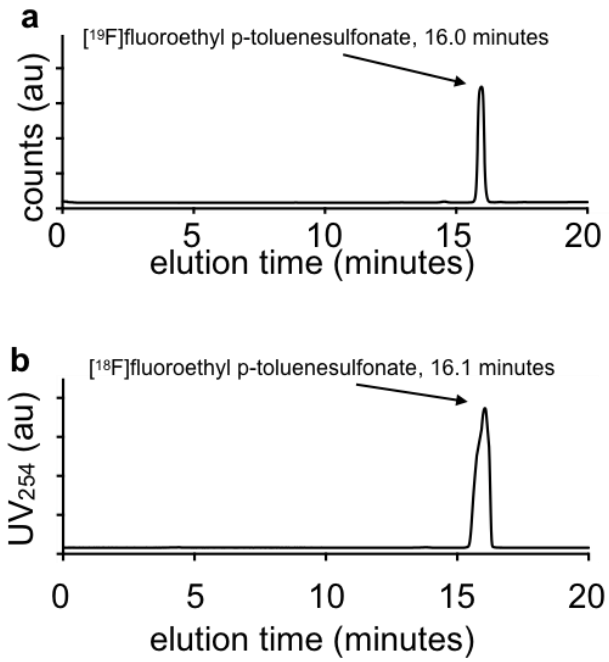

Fig. S9: QC chromatograms of (a) [^{19}F]fluoroethyl p-toluenesulfonate and (b) [^{18}F]fluoroethyl p-toluenesulfonate.

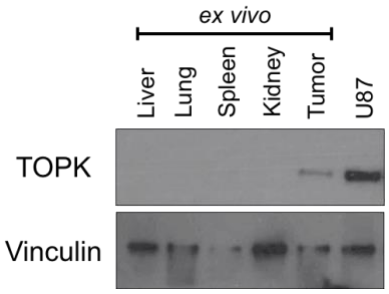

Fig. S10: Expression of human TOPK in murine *ex vivo* tissues, xenografts, and human cultured cancer cells. Vinculin is shown as a loading control.

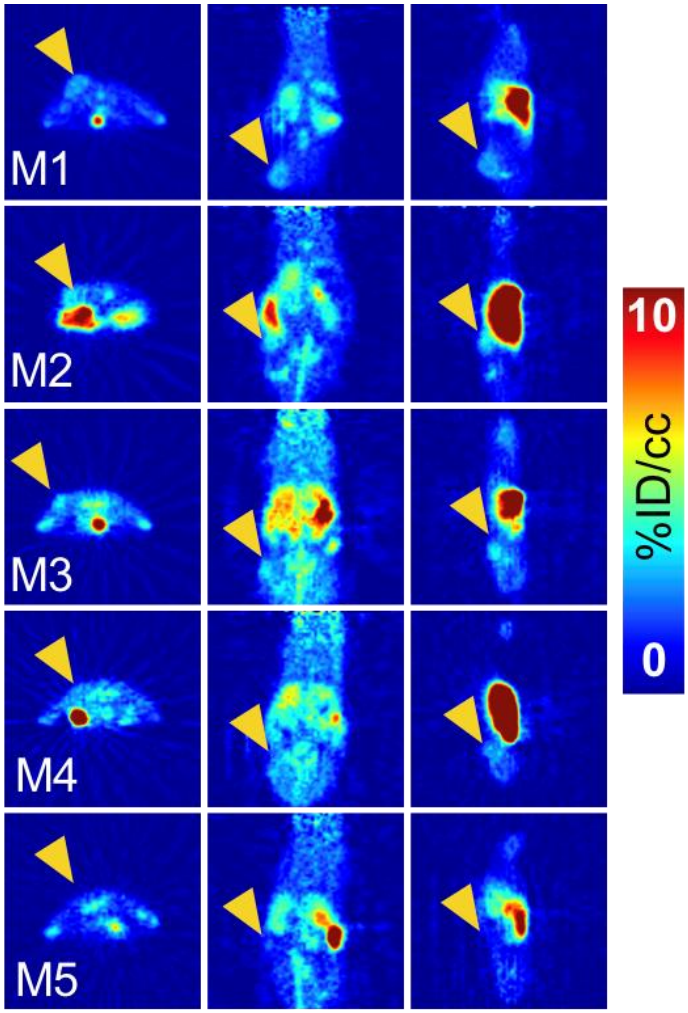

Fig. S11: PET slices for all mice. M1, M2, and M3 are unblocked. M4 and M5 are blocked with excess dose.

Table S1. Complete tabular PET VOI information					
Subject	**Volume (mm^3)**	**mean (%ID/cc)**	**SD (%ID/cc)**	**min (%ID/cc)**	**max (%ID/cc)**
M1	123.50	2.76	0.31	1.95	3.48
M2	67.42	3.05	0.51	1.87	4.59
M3	34.01	3.36	0.50	1.59	4.39
M4	34.01	1.70	0.95	-0.49	3.48
M5	70.40	1.10	0.77	-0.50	2.90

M1, M2, and M3 are unblocked. M4 and M5 are blocked with excess dose.

Table S2. Complete tabular biodistribution information (%ID/g)

organ	M1	M2	M3	M4	M5
blood	6.65	5.89	5.09	2.64	2.03
tumor	3.57	3.33	3.86	1.61	1.61
lung	2.89	8.71	0.42	2.04	2.11
heart	2.88	1.86	3.72	2.28	1.73
liver	4.17	5.98	6.70	4.24	2.90
spleen	12.32	16.07	19.65	15.93	7.70
small intestine	7.91	7.59	4.48	3.26	2.46
large intestine	5.23	4.38	4.58	6.29	1.89
stomach	2.86	3.47	3.42	2.62	2.93
kidney	4.81	5.90	6.06	3.46	3.25
muscle	1.37	1.86	1.79	1.37	1.22
skin	0.91	2.60	2.85	1.52	0.79
bone	3.26	1.86	17.92[a]	2.56	2.78

[a]Excluded as an outlier (maximum normalized residual - Grubb's - test).